A&A 384, 987–998 (2002)
DOI: 10.1051/0004-6361:20020061

Astronomy & Astrophysics

Mass-loss rates of H-rich central stars of planetary nebulae as distance indicators?

C. M. Tinkler[1] and H. J. G. L. M. Lamers[1,2]

[1] Astronomical Institute, University of Utrecht, Princetonplein 5, 3584CC, Utrecht, The Netherlands
[2] SRON Laboratory for Space Research, Sorbonnelaan 2, 3584CA, Utrecht, The Netherlands

Received 16 October 2001 / Accepted 14 January 2002

Abstract. If the mass loss rate, $\dot{M}$, or the modified wind momentum, Π, of central stars of planetary nebulae (CSPN) is strictly related to the luminosity, the study of their winds can be used to derive their distance as suggested in the literature. However, the mass loss rates and modified wind momenta of a sample of 13 CSPN published in the literature show a separation into two groups, which differ by a factor 10 to 10^2 in Π. This is partly, but not completely, due to differences in the adopted methods for mass loss determinations, and partly due to differences in the adopted stellar parameters, mainly the effective temperature. We have adopted a homogeneous set of stellar parameters, based on the Zanstra method, the dynamical ages of the nebulae and on evolutionary tracks, and scaled the mass loss rates accordingly. The revised data show that there is a large jump in $\dot{M}$ and Π near $T_{\rm eff} \simeq 60\,000$ K, with $\dot{M}$ and Π being larger by a factor 10 to 10^2 for the cooler group of CSPN of spectral type Of, than for the hotter group of type O. This discontinuity is most likely due to a bi-stability jump. The revised data do not show a clear relation between Π and the luminosity. The consequences are discussed in terms of the post-AGB evolution theory and the radiation driven wind models.

Key words. stars: distances – stars: early type – stars: evolution – stars: mass-loss – planetary nebulae: general

1. Introduction

Central stars of planetary nebulae (CSPN) of spectral type O have mass loss rates ($\dot{M}$) of order 10^{-8} to 10^{-6} $M_\odot$ yr^{-1} and terminal wind velocities of several thousands km s^{-1} (e.g. Kudritzki et al. 1997). The similarity between the wind properties of the hot CSPN and those of the much more massive Population I O-stars suggests that the winds of CSPN are driven by the same mechanism as those of massive O-stars, viz. radiation pressure by spectral lines. If that is the case, one may expect a relation between the "modified wind momentum", $\Pi = \dot{M} v_\infty {R_*}^{0.5}$, and the luminosity of the star (Kudritzki et al. 1995; Puls et al. 1996; Kudritzki & Puls 2000). For Pop I O-stars this relation has a small scatter of less than about a factor 2 in Π (Kudritzki & Puls 2000; Lamers et al. 2000). Kudritzki et al. (1999) have argued that the existence of such a tight relation between the modified wind momentum and the luminosity implies that the distance of the OBA stars can be derived from a study of their winds (see also Kudritzki & Puls 2000). If a similar relation also exists for CSPN stars, their luminosity could be derived from a study of their wind parameters.

Send offprint requests to: H. J. G. L. M. Lamers,
e-mail: lamers@astro.uu.nl

The determination of mass-loss rates of CSPN has been hampered by a poor knowledge of their stellar parameters, mainly the distance. Mass-loss rates determined by different authors sometimes differ by as much as a factor 10^2. This is partly due to differences in the adopted stellar parameters and partly due to differences in the methods used for the determination of $\dot{M}$.

Kudritzki et al. (1997) and Lamers & Cassinelli (1999, Chapt. 2) have shown that the modified wind momentum of 13 CSPN with mass loss rates derived by Perinotto (1993) and by Kudritzki et al. (1997) show a spread of about a factor 10^2 for the same luminosity. Is this due to uncertainties or errors in $\dot{M}$, or due to some other effect? If so, what is this effect? Kudritzki et al. (1997) suggested that differences in metallicity might play a role. They also pointed out that normal O-stars show a difference in the wind momentum versus luminosity relation between supergiants and main sequence stars and they suggested that the observed scatter for the CSPN may be due to the same effect.

In this paper we investigate the large scatter in $\dot{M}$ and in Π of the CSPN stars. We will concentrate on the H-rich O-type CSPN, i.e. we ignore the stars with a Wolf-Rayet type spectrum. We concentrate on the two samples of stars, studied by Perinotto (1993, hereafter called P93) and Kudritzki et al. (1997, hereafter called K97).

We investigate the differences in the stellar parameter adopted by these two groups and their effect on the determination of $\dot{M}$. We scale the mass loss rates to a common set of stellar parameters, and check if the resulting values of $\dot{M}$ and Π produce a smaller scatter in their relation on the stellar parameters. We will show that the mass loss rates of the hot CSPN ($T_{\rm eff} > 6 \times 10^4$ K) are significantly smaller than those of the cooler CSPN.

In Sect. 2 we briefly discuss the predicted relation between stellar luminosity and modified wind momentum. Section 3 deals with the stellar parameters adopted by P93 and K97 and with the more recent homogeneous data sample by Malkov (1997, 1998). In Sect. 4 we discuss the methods used to derive the mass-loss rates, the uncertainties incurred, and the scaling of these mass-loss rates to stellar parameters from Malkov (1997, 1998). These new mass-loss rates are treated individually in Sect. 5. In Sect. 6 we present the results of the search for dependencies between the mass-loss rates and stellar parameters. The results are discussed and the conclusions are presented in Sect. 7.

2. The modified wind momentum – Luminosity relation

The theory of line driven winds predicts that the mass-loss rate depends on stellar parameters as

$$\dot{M} \sim L_\star^{1/\alpha} M_{\rm eff}^{\frac{\alpha-1}{\alpha}} \tag{1}$$

and the terminal velocity of the wind scales as

$$v_\infty \sim v_{\rm esc} \sim \left(\frac{M_{\rm eff}}{R_\star}\right)^{0.5} \tag{2}$$

where $\alpha \simeq 0.5$ to 0.7 is a force multiplier parameter (Castor et al. 1975; Lamers & Cassinelli 1999; Kudritzki & Puls 2000). The effective mass is the mass corrected for the radiative force due to electron scattering. By combining (1) and (2) an expression for the *modified wind momentum* Π is obtained:

$$\Pi \equiv \dot{M} v_\infty R_\star^{0.5} \sim L_\star^{1/\alpha} M_{\rm eff}^{\frac{\alpha-1}{\alpha}+\frac{1}{2}}. \tag{3}$$

For a force multiplier parameter $\alpha \simeq \frac{2}{3}$ the modified wind momentum is practically independent of the effective mass. This is convenient since the effective mass is often an uncertain parameter.

Figure 1 shows the empirical relation between Π and luminosity for O-stars (data from Puls et al. 1996 and Lamers et al. 2002). The figure shows a tight relation with a slope of +1.53.

Figure 2 shows the empirical relation for the CSPN studied by P93 and K97, compared with the extrapolated relation of the Pop I O-stars. The data show a much larger scatter than the O-stars. There is even a hint for a separation into two groups of CSPN: those with a high Π and with much lower Π.

Comparing the data by P93 and K97, we see a systematic trend: Kudritzki's sample is located at higher wind momentum and at higher luminosity than Perinotto's sample. (Both samples will be discussed in detail below.) This trend is confirmed when looking only at the 3 stars P93 and K97 have in common: the central stars of NGC 6826, IC 4593, and IC 418. In all three cases the mass-loss rates, the modified wind momentum and the luminosities found by K97 (to be discussed below) are significantly higher than those found by P93. A likely explanation is the use of different stellar parameters by both authors and differences in the methods for determining the mass loss rates. *However, the difference in methods and in adopted parameters cannot be the only reason for the large scatter, because the K97 sample also contains four stars for which only an upperlimit of the mass loss rate and the modified wind momentum are known, and these limits are significantly below the relation defined by the other stars*

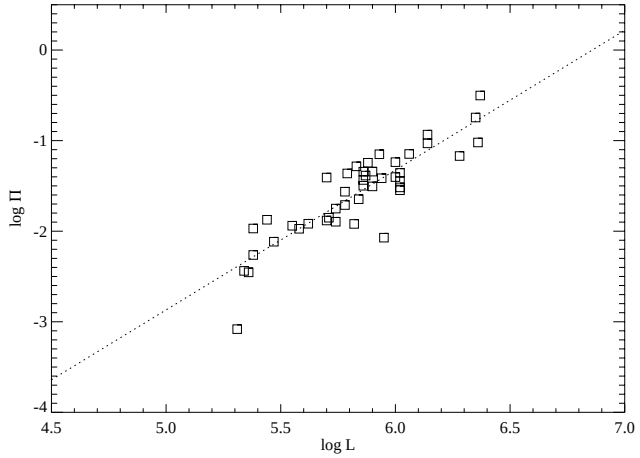

Fig. 1. Modified wind momentum (in $M_\odot$ yr^{-1} km s^{-1} ${R_\odot}^{0.5}$), versus luminosity (in $L_\odot$) of galactic O-stars. Data taken from Puls et al. (1996) and Lamers & Leitherer (1993), modified to take into account the optical depth effect.

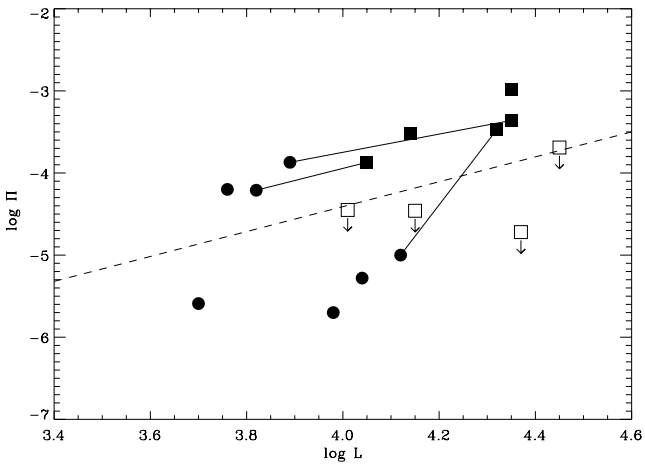

Fig. 2. Modified wind momentum (in $M_\odot$ yr^{-1} km s^{-1} ${R_\odot}^{0.5}$) versus luminosity (in $L_\odot$) of CSPN. Data by K97 are indicated by squares and those of P93 by circles. Upperlimits are indicated by open symbols. Full lines join the stars appearing in both samples. The dashed line is an extrapolation towards lower luminosities of the fit to galactic O-stars shown in Fig. 1.

in this sample. Similarly the P93 sample contains stars with high and with low values of Π.

It is interesting to note that the three stars of P93 with the smallest values of Π (NGC 1535, NGC 6210 and NGC 7009) are also the hottest stars of the sample (see later, Table 1). *This is an indication that the scatter or the separation may be due to a temperature effect.*

3. Stellar parameters

In this section we discuss the stellar parameters of CSPN adopted in the mass loss studies by Perinotto (1993), based on UV resonance lines, and by Kudritzki et al. (1997), based on the H and He lines. The parameters adopted by these authors show large differences, which affect their mass loss determinations. We also introduce the homogeneous set of parameters from Malkov (1997, 1998) that we will adopt for this study.

The stellar parameters, the mass loss rates ($\dot{M}$) and the modified wind momentum (Π) of the CSPN studied by P93 and K97 are listed in Table 1.

3.1. The Perinotto (1993) sample

From the mass-loss rates compiled by Perinotto (1993), which contains the stars studied by Perinotto et al. (1989) and Cerruti-Sola & Perinotto (1989), we include all except the central star of A78, which is a transitional object of the type [WC]-PG1159 (Werner & Koesterke 1992). This leaves a total of 7 CSPN. The effective temperature was taken equal to the Zanstra temperature, following the method developed by Bohlin et al. (1982). In the case of NGC 1535, NGC 7009, and IC 418, the adopted effective temperature was a 1:2 weighted average of the Zanstra temperature and the spectroscopic temperature derived by Mendez et al. (1988) who used photospheric line profiles (see Table 3).

The terminal velocity was taken equal to the edge velocity found from the P-Cygni profiles of the strongly saturated N V and/or C IV lines. The stellar radius was calculated in two ways: firstly from evolutionary tracks (computed by Schönberner (1981, 1983) and Wood & Faulkner (1986) in the $\log g$–$T_{\rm eff}$ diagram, and secondly from the relation between the terminal velocity of the wind v_∞, and the escape velocity $v_{\rm esc}$. The stellar mass of all CSPN was assumed to be equal to 0.6 $M_\odot$. This assumption was necessary to derive the stellar radius.

3.2. The Kudritzki et al. (1997) sample

In Kudritzki et al. (1997) stellar parameters and mass-loss rates of 9 CSPN were determined with a self-consistent spectroscopic method, using the unified model atmosphere code developed by Santolaya-Rey et al. (1997). Preliminary estimates of $T_{\rm eff}$, $\log g$, and the He abundance were derived by fitting optical H and He absorption lines using plane-parallel and hydrostatic NLTE models. The stellar mass was estimated from evolutionary tracks in the $\log g$–$T_{\rm eff}$ diagram. The stellar radius was calculated from the mass and $\log g$. Up to this point the method is nearly identical to the method used by Mendez et al. (1988). These preliminary estimates, combined with estimates of the mass-loss rate and velocity law exponent β (discussed later), were used to calculate new unified models, yielding improved theoretical profiles to other diagnostic lines. This fitting procedure was repeated until adequate fits were obtained to all stellar absorption and emission lines. The terminal velocity was determined from the P-Cygni profiles of UV resonance lines.

3.3. The adopted stellar parameters from Malkov (1997, 1998)

Malkov (1997, 1998, hereafter called "M97" for the two papers together) applied a self-consistent method for determining the distance, stellar parameters, and nebular optical depths to a large sample of CSPN, including all of the CSPN measured by P93 and K97 except for IC 4637. The method is based on choosing the distance such that the evolutionary age of the central star is equal to the dynamical age of its envelope. A comparison of the most recent individual distances found by various authors for the current sample is shown in Table 2. The several methods show a scatter of about a factor 2. Malkov's distances are generally a factor 1.5 lower than the spectroscopic distances derived by Mendez et al. (1992).

The stellar temperature was determined by Malkov in three ways: from Zanstra temperatures $T_{\rm Z}$(HeII) and $T_{\rm Z}$(HI), and by using the generalized energy-balance method described in Malkov et al. (1995). The latter method is based on the energy-balance method as formulated by Preite-Martinez & Pottasch (1983), and includes the energy losses caused by unobservable collisional excitation of neutral hydrogen and helium, without which the central star temperature may in some cases be underestimated by up to 0.5 dex.

The He II Zanstra temperature could only be determined for hotter stars (above 50 000 K) with measurable He II lines. For cooler stars with optically thick nebulae (NGC 6543 and IC 418) $T_{\rm Z}$(HI) was used, while for NGC 6826, IC 4593, He 2-108, and He 2-131 $T_{\rm GB}$ (generalized energy-balance method) was used. Tylenda et al. (1994) argued that, in most cases, the Zanstra discrepancy between $T_{\rm Z}$(He II) and $T_{\rm Z}$(H I) is due to the fact that the nebulae are optically thin in the Lyman continuum of hydrogen, causing $T_{\rm Z}$(H I) to be underestimated. This is confirmed quantitatively by Gruenwald & Viegas (2000), who show that for temperatures below 100 000 K $T_{\rm Z}$(He II) generally gives a good value for the effective stellar temperature, and that the Zanstra discrepancy disappears for optically thick nebulae.

The effective temperatures derived by M97 are compared with the temperatures adopted by P93 and K97 and with the spectroscopic temperatures from Mendez et al. (1992) in Table 3. The temperatures adopted in this study,

Table 1. Stellar parameters and derived mass loss rates.

Object	Spectral type	$T_{\rm eff}$ (kK)	$R_\star$ ($R_\odot$)	$\log L_\star/L_\odot$	$M_\star$ ($M_\odot$)	v_∞ (km s^{-1})	$\log \dot{M}$ ($M_\odot$/yr)	$\log \Pi$ ($M_\odot$/yr km s^{-1} $R_\odot^{0.5}$)
NGC 6826	O3f(H)	45	1.45	3.89	0.60	1750	−7.19	−3.87
IC 4593	O5f(H)	35	2.20	3.82	0.60	1000	−7.38	−4.21
IC 418	Of(H)	37	2.80	4.12	0.60	940	−8.20	−5.00
NGC 1535	O(H)	77	0.55	3.98	0.60	1900	−8.85	−5.70
NGC 6210	O(H)	90	0.29	3.70	0.60	2180	−8.66	−5.59
NGC 6543	Of-WR(H)	60	0.70	3.76	0.60	1900	−7.40	−4.20
NGC 7009	O(H)	88	0.45	4.04	0.60	2770	−8.55	−5.28
NGC 6826	O3f(H)	50	2.00	4.35	0.91	1200	−6.59	−3.36
IC 4593	O5f(H)	40	2.20	4.05	0.70	900	−7.00	−3.87
IC 418	Of(H)	37	3.50	4.32	0.90	700	−6.59	−3.47
He 2-108	Of(H)	35	3.20	4.14	0.74	700	−6.62	−3.52
He 2-131	Of(H)	30	5.50	4.35	0.89	500	−6.05	−2.98
NGC 2392	Of(H)	45	2.50	4.37	0.92	400	<−7.52	<−4.72
NGC 3242	O(H)	75	0.60	4.01	0.65	2300	<−7.70	<−4.45
IC 4637	O(H)	55	1.30	4.15	0.78	1500	<−7.70	<−4.46
Tc 1	Of(H)	33	5.10	4.45	0.96	900	<−7.00	<−3.69

Top: stars studied by P93. Below: stars studied by K97.
The first three stars are in both samples.

Table 2. Comparison of distances (in kpc).

Object	$d_{\rm M}$ (1)	$d_{\rm S}$ (2)	$d_{\rm exp}$ (3)	$d_{\rm ext}$ (4)	$d_{\rm H}$ (5)
NGC 6826	1.6	1.9			
IC 4593	2.1	3.2			
IC 418	1.2	1.6			
NGC 1535	1.3	2.0			
NGC 6210	3.1		1.57		
NGC 6543	1.8		1.00*		
NGC 7009	1.6	2.1			
He 2-108	3.2	6.0		>3.0	
He 2-131	2.2			2.8	
NGC 2392	0.9	2.0	1.60		1.5:
NGC 3242	1.2	1.8	0.51		
Tc 1	2.2	3.3		2.8	

(1) Self-consistent distance, Malkov (1997, 1998).
(2) Spectroscopic distance, Mendez et al. (1992).
(3) Expansion distance, Terzian (1997), * Reed et al. (1999).
(4) Extinction distance, Martin (1994).
(5) Hipparcos distance, highly uncertain, Acker et al. (1998).

$T_{\rm eff}$, (last column) are roughly in agreement with the ones adopted by P93 and K97, except for a few large differences: NGC 6826, NGC 6210 and NGC 6543 have $T_{\rm eff}$ considerably smaller than adopted by P93, whereas NGC 2392 and NGC 3242 have $T_{\rm eff}$ considerably higher than adopted by K97. (The stars will be discussed individually in Sect. 5.)

The masses, radii, and luminosities were derived by M97 from the distance and the relationship between $T_{\rm eff}$ and $\log g$ using evolutionary tracks from Schönberner (1981, 1983) and Blöcker (1995). The stellar parameters of the program stars, derived by M97, are listed in Table 4.

4. Observed and scaled mass-loss rates

In this section we describe the methods used for the determinations of the mass loss rates by P93 and K97. We then correct these values by adopting the stellar parameters from M97. The results will be called $\dot{M}_{\rm scaled}$.

4.1. Mass loss rates of Perinotto's (P93) sample

The mass loss rates of the P93 sample of CSPN were derived from a study of the P Cygni profiles of UV resonance lines, using the SEI line-fit method (Lamers et al. 1987). Nebular abundances ($A_{\rm E}$), taken from various authors, were adopted. The mass-loss rate was calculated as follows:

$$\dot{M} = 1.23\times10^{-8}\frac{(R_\star/R_\odot)v_\infty^2\,(\mathrm{km\,s^{-1}})}{f\lambda_0(\dot{A})A_{\rm E}}\frac{Z}{q_iU_i} \qquad (4)$$

where f is the oscillator strength of the transition, and λ_0 is the rest wavelength of the line. Z contains the velocity law and line optical depths as determined from the line fitting. The excitation fraction U_i can be expressed as

$$U_i = W\frac{g_{i,\rm l}}{g_{i,\rm o}}\exp\left(\frac{-E_{\rm l,g}}{kT_{\rm exc}}\right), \qquad (5)$$

where $g_{i,\rm o}$ and $g_{i,\rm l}$ are the statistical weights of the ground level and of the lower level of the observed transition, respectively; $E_{\rm l,g}$ is the energy of the lower level of the observed transition, and $T_{\rm exc}$ is the excitation temperature at the wavelength corresponding to the energy is $E_{\rm l,g}$. P93 adopted $T_{\rm exc} = T_{\rm eff}$.

The ionization fraction $q_{\rm i}$ of the observed ions is derived empirically from the O IV and O V resonance lines. P93 argued that O IV and O V together should account for almost all O in the wind. So, by setting the sum of

Table 3. Comparison of derived effective temperatures (in kK).

Object	$T_{\rm P}$ (1)	$T_{\rm K}$ (2)	$T_{\rm S}$ (3)	$T_{\rm Z}$(HeII) (4)	$T_{\rm Z}$(HeII) (5)	$T_{\rm Z}$(HI) (6)	$T_{\rm GB}$ (7)	τ (8)	$T_{\rm eff}$ (9)
NGC 6826	45	50	50			34.4	40.0	1.2	40.0
IC 4593	35	40	40	50		32.4	40.9	0.49	40.9
IC 418	37	37	36			38.0	37.3	>100	38.0
NGC 1535	77		70	68	80.8	38.9	71.0	0.32	80.8
NGC 6210	90			69	54.8	47.3	57.9	3.7	54.8
NGC 6543	60					47.2	42.7	>100	47.2
NGC 7009	88		82	84	88.7	59.8	69.9	2.4	88.7
He 2-108		35	33	52		31.2	34.5	0.85	34.5
He 2-131		30				33.4	33.4	>100	33.4
NGC 2392		45	47	67	73.7	32.7	89.7	0.11	73.7
NGC 3242		75	75	91	94.5	53.3	86.2	1.2	94.5
Tc 1		33	33			32.4	35.2	3.1	33.8

(1) Effective temperatures adopted by P93 (Zanstra/spectroscopic).
(2) Effective temperatures adopted by K97 (spectroscopic).
(3) Spectroscopic temperatures, Mendez et al. (1992).
(4) HeII Zanstra temperatures, Preite-Martinez (1993).
(5) HeII Zanstra temperatures, Malkov (1997, 1998).
(6) HI Zanstra temperatures, Malkov (1997, 1998).
(7) Generalized energy balance temperatures, Malkov (1997, 1998).
(8) Nebular optical depth within the neutral hydrogen ionization region (Malkov 1997, 1998).
(9) Adopted effective temperatures.

Table 4. Revised stellar parameters and mass loss rates.

Object	Spectral type	$T_{\rm eff}$ (kK)	$R_\star$ ($R_\odot$)	$\log L_\star/L_\odot$	$M_\star$ ($M_\odot$)	$\log g$	v_∞ (km s^{-1})	$\log \dot{M}_{\rm scaled}$ ($M_\odot$/yr)	$\log \Pi$ ($M_\odot$/yr km s^{-1} $R_\odot^{0.5}$)
NGC 6826	O3f(H)	40.0	1.45	3.69	0.586	3.88	1750	-6.1 ± 0.7	-2.8 ± 0.7
IC 4593	O5f(H)	40.9	1.40	3.70	0.588	3.91	1000	-7.3 ± 0.7	-4.2 ± 0.7
IC 418	Of(H)	38.0	1.64	3.68	0.584	3.77	940	-7.8 ± 0.7	-4.8 ± 0.7
NGC 1535	O(H)	80.8	0.38	3.76	0.605	5.05	1900	-8.7 ± 0.7	-5.6 ± 0.7
NGC 6210	O(H)	54.8	0.81	3.73	0.596	4.39	2180	-7.0 ± 0.7	-3.7 ± 0.7
NGC 6543	Of-WR(H)	47.2	1.00	3.65	0.580	4.20	1600	-6.1 ± 0.7	-2.9 ± 0.7
NGC 7009	O(H)	88.7	0.34	3.81	0.619	5.16	2770	-8.3 ± 0.7	-5.1 ± 0.7
NGC 6826	O3f(H)	40.0	1.45	3.69	0.586	3.88	1200	-6.5 ± 0.5	-3.3 ± 0.5
IC 4593	O5f(H)	40.9	1.40	3.70	0.588	3.91	900	-7.3 ± 0.5	-4.3 ± 0.5
IC 418	Of(H)	38.0	1.64	3.68	0.584	3.77	700	-7.1 ± 0.5	-4.2 ± 0.5
He 2-108	Of(H)	34.5	1.65	3.52	0.563	3.75	700	-7.0 ± 0.5	-4.1 ± 0.5
He 2-131	Of(H)	33.4	2.36	3.78	0.602	3.47	500	-6.9 ± 0.5	-3.9 ± 0.5
NGC 2392	Of(H)	73.7	0.61	3.99	0.673	4.69	400	<-9.1	<-6.6
NGC 3242	O(H)	94.5	0.28	3.75	0.607	5.31	2300	<-8.5	<-5.4
Tc 1	Of(H)	33.8	1.88	3.59	0.566	3.64	900	<-7.7	<-4.6

Upper part = P93 sample; Lower part = K97 sample.
The first three stars are in both samples.

the O IV and O V column densities to the total column density of O, the mean ionization fractions of these two ions are known. In the case of NGC 1535, NGC 6210, and NGC 7009, where only the O V line could be used to determine the mass-loss rate, Perinotto argues that O V is probably greater than 0.25 for two reasons:

1. O VI is unlikely to be the main ionization stage of oxygen (the ionization energy of O V is 113.9 eV);
2. These stars are somewhat hotter than NGC 6543 and NGC 6826, for which $q(\mathrm{O\,V}) \simeq 0.1$ was derived.

By adopting $q(\mathrm{O\,V}) = 0.5$ Perinotto therefore expects the resulting uncertainty in the mass-loss rate to be within a factor 2. For IC 418 and IC 4593 the mass loss rates are based on a study of the N V lines.

The nebular abundances, adopted by P93, may be different from the abundances in the wind. Moreover, recent

more accurate nebular abundance determinations using infrared spectroscopy indicate that while errors in previous O abundances are usually around 30%, previous C and N nebular abundances are often in error by about a factor 2 (Pottasch, private communication).

The mass-loss rates from UV P-Cygni profiles as determined by P93 depend exponentially on the excitation temperature, making this parameter the most crucial one. P93 adopted $T_{\rm exc} = T_{\rm eff}$. Probably a more realistic value, adopted by K97, is $T_{\rm rad} \simeq 0.77\ T_{\rm eff}$. Adopting this would raise the mass loss rates of P93 by about a factor 3. Using the new values of the effective temperatures produces an additional correction.

We have corrected the mass loss rates of the P93 sample of CSPN for the improved stellar parameters as given in Table 4, and for the improved estimate of the excitation temperature. The resulting values of $\dot{M}$ and Π are listed in the last columns of Table 4. We conservatively estimate the uncertainty in these mass loss rates to be about a factor five, mainly due to the uncertainties in the abundances and the ionization and excitation fractions.

4.2. Mass loss rates of Kudritzki's (K97) sample

The mass loss rates from the K97 sample are based on a study of the H and He II lines, using unified model atmospheres to determine both $\dot{M}$ and the stellar parameters. The mass-loss rate and velocity law exponent β are estimated from fits to the stellar Hα emission profile according to the method derived by Puls et al. (1996). The velocity law used is:

$$v(r) = v_\infty(1 - (b/r))^\beta \tag{6}$$

where b is a constant selected to yield a prespecified velocity of $0.1 v_{\rm sound}$ at the transition from the hydrostatic to the hydrodynamic regime.

The mass-loss rate derived from the Hα profile depends on the stellar parameters as

$$\dot{M}_{H_\alpha} \sim R_\star^{3/2} v_\infty^{5/3} \frac{\Delta\exp}{T_{\rm eff}^{3/2}} \tag{7}$$

with

$$\Delta\exp = \exp\left(\frac{5.184}{T_{\rm eff}}\right) - \exp\left(\frac{2.337}{T_{\rm eff}}\right) \tag{8}$$

(see Puls et al. 1996).

The main source of uncertainty in the mass loss rates of the K97 sample is probably the spectroscopic stellar radius, due to the well known surface gravity problem in the analysis of the Hγ line. Pottasch & Acker (1998) show that in three CSPN, for which the Hipparcos satellite has measured the distance, the derived surface gravities are considerably higher than the spectroscopically determined surface gravities. It is therefore not unlikely that for some or all of the CSPN studied by Kudritzki the (spectroscopic) stellar radii, and consequently the mass-loss rates, have been overestimated.

An additional source of uncertainty in the mass loss rate is due to the sensitivity of the emission line profiles to the details of the shape of the velocity law since the emissivity depends on ρ^2 and $\rho(r) \sim r^{-2} v(r)^{-1}$. Puls et al. (1996) showed that in the Hα analysis an error of 30% in the exponent β of the velocity law can lead to an error of up to a factor 2.8 in the mass-loss rate, although this error should be reduced by the fact that β affects the *profile* of the Hα line as well as the equivalent width (the larger β, the higher the central part of the Hα emission component). See also the critical discussion by Kudritzki & Puls (2000).

We have corrected the mass loss rates of the K97 sample for the improved stellar parameters, listed in Table 4. The resulting values of $\dot{M}$ and Π are given in the last columns of Table 4. We conservatively estimate the uncertainty of $\dot{M}$ to be about a factor 3, mainly because of the uncertainty in the velocity law and radius.

The new values of $\dot{M}$ and Π are compared with the old ones in Fig. 3. In general the new values of the P93 sample are larger than the original ones, whereas those of the K97 sample are smaller. For three stars of the P93 sample the new values are an order of magnitude larger than the original ones. These are NGC 6826, NGC 6210 and NGC 6543. The star of the K97 sample that has the largest correction is He 2-131.

5. Discussion of each individual star

On average, the new scaled mass-loss rates $\dot{M}_{\rm scaled}$ are lower than the K97 mass-loss rates, due to the smaller stellar radii derived by M97, and higher than the P93 mass-loss rates, due to the reduction in the radiation temperature $T_{\rm rad} = 0.77\ T_{\rm eff}$. In some cases, however, the stellar parameters derived by M97 are very different from those dopted by P93 and K77, and the mass-loss rate changed drastically. The main reason for this is that the stellar radius is strongly dependent on the stellar temperature due to the use of evolutionary tracks: a lower value of $T_{\rm eff}$ automatically leads to a higher radius, and vice versa. This affects the derived the mass-loss rate. We discuss each star individually, in alphabetical order.

- **NGC 1535**: $\log \dot{M}_{\rm scaled} - \log \dot{M}_{\rm P93} = 0.15$
  The parameters for this star are nearly the same before and after the scaling.
- **NGC 2392**: $\log \dot{M}_{\rm scaled} - \log \dot{M}_{\rm K97} = -1.6$
  The large difference is due to the large increase in $T_{\rm eff}$ from 45 000 K (K97) to 73 700 K (M97) and the corresponding decrease in radius from 2.5 to 0.61 $R_\odot$. Mendez et al. (1988) argued that the presence of He I absorptions at λ4471 and λ4713 implies that $T_{\rm eff}$ can not be much higher than 50 kK. However, Malkov et al. (1995) point out that strong emission lines of highly ionized species are present in the nebular spectrum that are inconsistent with the low temperature found by Mendez et al. (1988). The He II Zanstra temperature derived by Preite-Martinez (1993) and the

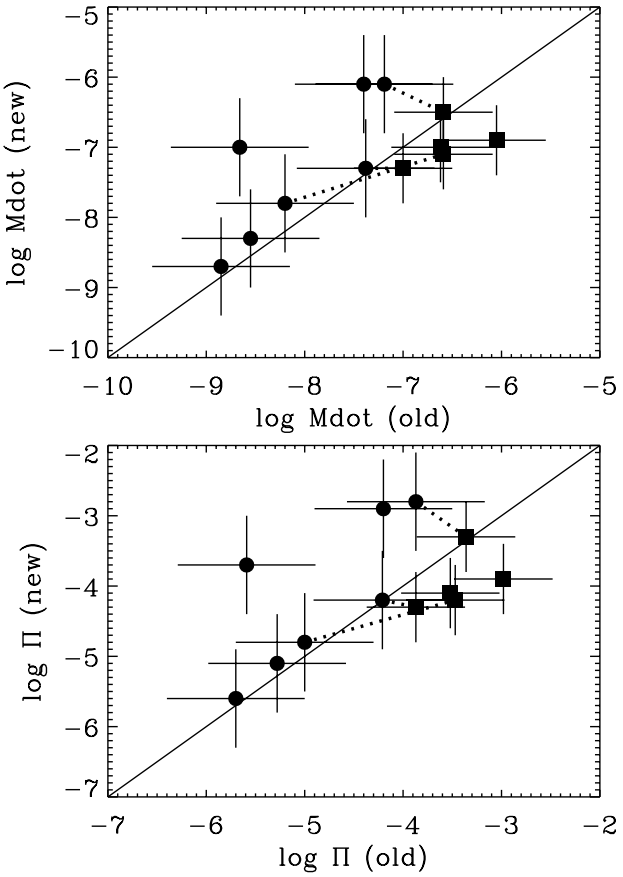

Fig. 3. The scaled mass loss rates and the scaled modified wind momenta versus the original ones in the upper and lower figure respectively. Circles and squares indicate stars of the P93 and K97 samples respectively. The scaled values of the P93 sample are larger than the original ones, whereas those of the K97 sample are smaller than the original ones. Data from the same star in both samples are connected by a dotted line.

generalized energy-balance temperature derived by Malkov (1997) both support the higher temperature.

As seen in Table 2 the distance to NGC 2392 has recently been determined in four different ways, including a Hipparcos measurement of the trigonometric parallax yielding a distance of 1.5 kpc (Acker et al. 1998). The uncertainty in the parallax is very large though, resulting in an estimated minimum value as low as 0.2 kpc. The expansion distance given by Terzian (1997) is 1.6 kpc, and in an earlier article Haijan et al. (1995) derived a lower limit to this distance of 1.4 kpc. The expansion distances in Table 2 are generally lower than the distance found by M97 by about a factor 2. However, for NGC 2392 M97 derived the smaller distance of 0.92 kpc. Possibly this distance is underestimated, which would explain in part why the difference in stellar radii and temperature between K97 and M97 is so unusually large.

NGC 2392 has quite extreme properties compared with the rest of the sample:

- The stellar mass derived by M97 is the highest of the sample (Table 4).
- NGC 2392 is the only planetary nebula in this sample that is classified by Perinotto (1991) as type I, due to its high N/O abundance ratio. This, in combination with a relatively low C/O ratio, is perfectly consistent with a higher mass AGB precursor (Iben 1995).
- The nebula has the smallest optical thickness (Table 2).
- The derived nebular expansion velocity of 52.5 $\mathrm{km\,s^{-1}}$ is anomalously high (M97).
- The ratio between the $v_\infty/v_{\rm esc} = 0.76$ is abnormally small.

Obviously the central star of NGC 2392 is very unusual.

- **NGC 3242**: $\log \dot{M}_{\rm scaled} - \log \dot{M}_{\rm K97} = -0.8$
  The adopted He II Zanstra temperature of 94 kK derived by M97 is higher than the spectroscopic temperature of 75 kK adopted by K97. This results in a lower value of the upper limit of the mass-loss rate.
- **NGC 6210**: $\log \dot{M}_{\rm scaled} - \log \dot{M}_{\rm P93} = +1.7$
  Very different Zanstra temperatures are found by P93 (90 kK) and by M97 (55 kK). Preite-Martinez (1993) found a value in between, $T_{\rm Z}({\rm HeII}) = 69$ kK. Combined with the resulting difference in R_*, and of course the lower value of $T_{\rm rad}$, this results in an increase of the the mass-loss rate of nearly a factor 50.
- **NGC 6543**: $\log \dot{M}_{\rm scaled} - \log \dot{M}_{\rm P93} = +1.3$
  The lower temperature derived by M97 implies a large increase in the mass-loss rate. This star was also analyzed by de Koter et al. (1996), who found a very similar stellar effective temperature as M97 of 47 kK. The mass loss rate is high, which is not surprising considering its spectral type of Of-WR.
- **NGC 6826**: $\log \dot{M}_{\rm scaled} - \log \dot{M}_{\rm P93} = +0.7$ and $\log \dot{M}_{\rm scaled} - \log \dot{M}_{\rm K97} = +0.1$
  According to Mendez et al. (1990) the central star of NGC 6826 is "almost" of spectral type Of-WR. This agrees with its high mass loss rate.
- **NGC 7009**: $\log \dot{M}_{\rm scaled} - \log \dot{M}_{\rm P93} = +0.2$
  No significant change in the stellar parameters, nor in the mass loss rate.
- **He 2-108**: $\log \dot{M}_{\rm scaled} - \log \dot{M}_{\rm K97} = -0.4$
  The reduction in the radius from 3.2 (K97) to 1.65 (M97) $R_\odot$ results in a decrease of the mass loss rate.
- **He 2-131**: $\log \dot{M}_{\rm scaled} - \log \dot{M}_{\rm K97} = -0.7$
  The reduction in the radius from 5.5 (K97) to 2.4 (M97) $R_\odot$ results in a decrease of the mass loss rate.
- **IC 418**: $\log \dot{M}_{\rm scaled} - \log \dot{M}_{\rm P93} = +0.4$ and $\log \dot{M}_{\rm scaled} - \log \dot{M}_{\rm K97} = -0.5$
  The large difference in the mass-loss rates of P93 and K97 of 1.6 dex has decreased to 0.7 dex due to the scaling to the M97 stellar parameters.
- **IC 4593**: $\log \dot{M}_{\rm scaled} - \log \dot{M}_{\rm P93} = +0.1$ and $\log \dot{M}_{\rm scaled} - \log \dot{M}_{\rm K97} = -0.3$
  The changes in the stellar parameters and in the mass loss rates are small for this star.
- **Tc 1**: $\log \dot{M}_{\rm scaled} - \log \dot{M}_{\rm K97} = -0.7$
  The stellar radius of 5.1 $R_\odot$ (K97) was reduced to

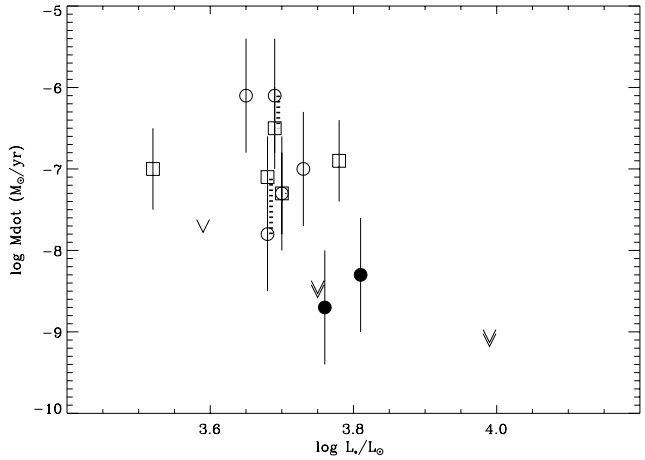

Fig. 4. The scaled mass loss rates versus luminosity. Circles and squares indicate the scaled rates of the P93 and K97 samples respectively. Data from the same star in both samples are connected by dotted lines. Arrows indicate upperlimits from the K97 sample. Open symbols and single arrows are stars with $T_{\rm eff} < 60\,000$ K; filled symbols and double arrows are stars with $T_{\rm eff} > 60\,000$ K. Notice that the hottest stars have the smallest mass loss rates and the lowest upper limits.

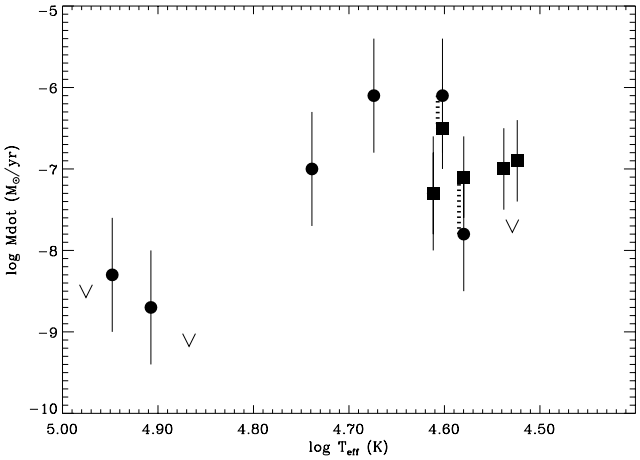

Fig. 5. The scaled mass loss rates versus effective temperature. Circles and squares indicate the scaled rates of the P93 and K97 samples respectively. Data from the same star in both samples are connected by a dotted line. Arrows indicate upperlimits from the K97 sample. Notice that the mass loss rates increase with decreasing $T_{\rm eff}$.

1.9 $R_\odot$ by M97. This results in a reduction of the upper limit.

6. The dependence of $\dot{M}$ and Π on the stellar parameters

6.1. The mass loss rate, $\dot{M}$

Figure 4 shows the dependence of $\dot{M}$ on luminosity. At first sight this figure shows a general trend of *decreasing* $\dot{M}$ towards higher luminosity. This is surprising, because the radiation driven wind theory predicts that $\dot{M}$ *increases* with luminosity. Therefore we have used different symbols for different ranges of $T_{\rm eff}$. We see that the stars with $T_{\rm eff} > 60\,000$ K have the smallest mass loss rates. This suggests that the mass loss rate depends on both L_* and $T_{\rm eff}$. This is shown in Fig. 5. Here we very clearly see a split of the sample into two groups: stars with $T_{\rm eff} < 60\,000$ K have much higher mass loss rates than those with $T_{\rm eff} > 60\,000$ K.

In order to determine the dependence of $\dot{M}$ on the stellar parameters, we have calculated weighted linear regression relation of the type

$$\log \dot{M} = a_0 + a_1 \times \log L_* + a_2 \times \log \left(T_{\rm eff}/10^3\right). \qquad (9)$$

We find $a_0 = +0.05$, $a_1 = -0.45 \pm 2.58$, $a_2 = -3.37 \pm 1.63$. This relation fits the data with an accuracy of $1\sigma = 0.51$, which is about as large as the error in the empirical mass loss rate. The small value of a_1 and its large uncertainty shows that the mass loss rate depends mainly on $T_{\rm eff}$ and only little on L_*. This is confirmed by the simpler fit relation

$$\log \dot{M} = -1.39 - 3.50\ (\pm 1.43) \times \log \left(T_{\rm eff}/10^3\right) \qquad (10)$$

which fits the data equally well ($1\sigma = 0.52$). The upper limits agree with this relation. We have also tried other linear regression relations including the stellar radius or mass, but these did not result in a more accurate description of $\dot{M}$. We conclude that the mass loss rate of CSPN depends most strongly on the effective temperature of the stars, and only little on the luminosity.

6.2. The modified wind momentum Π

Figure 6 shows the relation between Π and L_*. The two groups of CSPN measured by P93 and K97 are now intermingled in a narrower luminosity range but in a larger range in Π compared to Fig. 2. Before scaling, the stars seemed to be divided into a strong wind and a weak wind group. Each group showed the general trend of an increase in Π with increasing L_*, as predicted by the radiation driven wind theory. The data do no longer show such a relation between Π and L_*. This is due to the changes in adopted stellar parameters such as effective temperature. This is shown in Fig. 6 by the different symbols for stars with $T_{\rm eff}$ higher or lower than 60 000 K. The hottest group has clearly the smallest values of Π. Comparing the result with the extrapolated Π versus L_* relation of the O-stars, we find that the values of Π for the hottest stars are below this relation whereas those of the cooler group are above the relation.

We have derived expressions for the modified wind momentum, Π, as a function of luminosity and temperature of the type

$$\log \Pi = b_0 + b_1 \times \log L_* + b_2 \times \log \left(T_{\rm eff}/10^3\right). \qquad (11)$$

We find with a weighted linear regression method that $b_0 = 0.98$, $b_1 = -0.07 \pm 2.58$, $b_3 = -2.93 \pm 1.63$. This expression fits the data with an accuracy of $1\sigma = 0.61$. The small value of b_1 and its large uncertainty suggests

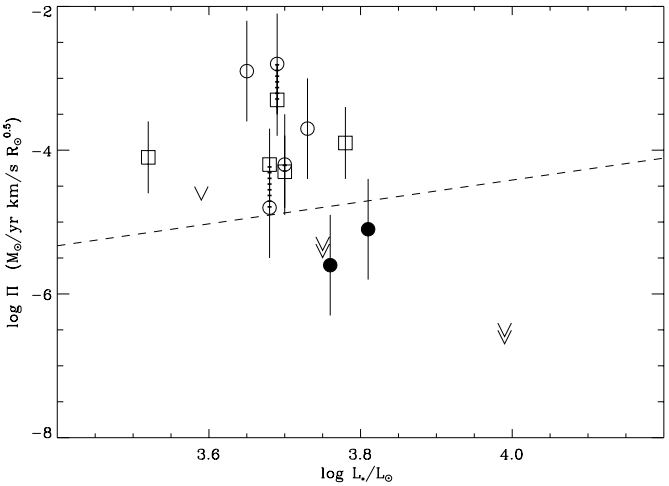

Fig. 6. Modified wind momentum versus luminosity of CSPN, calculated with the new mass loss rates and stellar parameters. Circles and squares refer to the P93 and K97 samples respectively. Arrows indicate upper limits. Open circles and single arrows are stars with $T_{\rm eff} < 60\,000$ K; filled symbols and double arrows are stars with $T_{\rm eff} > 60\,000$ K. Data from the same star in both samples are connected by dotted lines. The hottest stars have the smallest values of Π. The dashed line is an extrapolation towards lower luminosities of the fit to galactic O-stars shown in Fig. 1.

that Π depends mainly on $T_{\rm eff}$. Indeed, if we describe Π as a function of $T_{\rm eff}$ only we find.

$$\log \Pi = +0.77 - 2.95\ (\pm 1.43) \times \log\left(T_{\rm eff}/10^3\right) \qquad (12)$$

with the same scatter of $1\sigma = 0.61$. This scatter is about the same as the mean uncertainty in the empirical values of Π. The upper limits agree with this relation. We have also tried other linear regression relations including the stellar radius or mass, but these did not result in a more accurate description of Π. We conclude that Π depends mostly on $T_{\rm eff}$.

6.3. A bi-stability jump for CSPN

Lamers et al. (1995) have shown empirically that the stellar wind properties of hot stars show bi-stability jumps near $T_{\rm eff} \simeq 21\,000$ K and near 10 000 K. At these jumps the terminal wind velocity drops steeply by about a factor two and the mass loss rate increases steeply by about a factor three to five, when going from high to low temperatures (Lamers et al. 1995; Vink et al. 1999). Vink et al. (1999), in their theoretical study of mass loss rates, have shown that these jumps are due to changes in the radiative line-driving at low velocities (near the sonic point) when the ionization of the dominant driving element (Fe) flips to a higher or lower stage. Vink et al. (2001) have also predicted that additional bi-stability jumps may occur at higher temperatures where CNO may provide the dominant line driving, especially for low metallicity stars.

The scaled mass loss rates derived in this paper suggest the occurence of a jump somewhere between 55 000 and 70 000 K (Fig. 5). If such a jump indeed occurs, the description of the mass loss rate in terms of one single dependence of $\dot{M}$ or Π over the full temperature range is meaningless. Therefore we have also derived linear regressions for $\dot{M}$ and Π as a function of L_* and $T_{\rm eff}$ for the sample of ten stars with $T_{\rm eff} < 60\,000$ K. We find that even for this subsample $\dot{M}$ and Π are best described by a single dependence on $T_{\rm eff}$ and not on L_* or a combination of L_* and $T_{\rm eff}$. We find that the best relations are

$$\log \dot{M} = -9.44 + 1.58\ (\pm 3.30) \times \log\left(T_{\rm eff}/10^3\right) \qquad (13)$$

with $1\sigma = 0.44$,

$$\log \Pi = -9.22 + 3.36\ (\pm 3.30) \times \log\left(T_{\rm eff}/10^3\right) \qquad (14)$$

with $1\sigma = 0.51$ and

$$\log \Pi = -6.03 + 0.59\ (\pm 2.56) \times \log(L_*) \qquad (15)$$

with $1\sigma = 0.54$, all for $T_{\rm eff} < 60\,000$ K.

We see that both Π and $\dot{M}$ of this subsample depend on a positive power of $T_{\rm eff}$ (although the uncertainty is large), whereas the full sample showed a negative power (Eqs. (11) and (12)). Similarly, we find that Π depends on a positive power of L_*, as predicted, but again with a large uncertainty in the coefficient.

If we compare these fits with a simple mean value of $\dot{M}$ and Π we find $<\log \dot{M}> = -6.91 \pm 0.51$ and $<\log \Pi> = -3.82 \pm 0.61$. We see that the 1σ values of these assumed constant values are hardly larger than those of their relation with $T_{\rm eff}$.

7. Discussion, conclusions and consequences

7.1. Discussion and conclusions

We have shown that the mass loss rates and the modified wind momentum derived from the UV lines from excited levels of O V and O IV or from the emission lines (Hα, He I or He II) depend very strongly on the adopted stellar parameters. The most crucial parameter is $T_{\rm eff}$. The mass loss rates derived from the emission lines are proportional to $\Delta \exp \times {T_{\rm eff}}^{-3/2}$ (see Eqs. (7) and (8)). The mass loss rates derived from the UV lines from excited levels depend on $T_{\rm eff}$ via the the adopted ionization and excitation fractions (see Eqs. (4) and (5)). Uncertainties in the adopted radius of the star also affects the mass loss determinations. This is especially the case if the radius is determined from $T_{\rm eff}$ and the luminosity, because in that case an error in $T_{\rm eff}$ also introduces an error an R_*. Part of the large differences in derived mass loss rates between the samples from K97 and P93 is due to differences in the adopted stellar parameters, mainly $T_{\rm eff}$. Additional errors may be introduced by uncertainties in the procedure used for fitting the theoretical line profiles to the observed ones and, in case the UV lines are used, also by uncertainties in the adopted abundances (see Sect. 4.1).

We have tried to improve the situation by adopting one homogeneously derived set of stellar data from M97, in which the Zanstra temperatures, the dynamical age and the predicted evolutionary tracks are all taken into account. For some CSPN this leads to drastically different values from the ones adopted by P93 or K97 (see Table 3). The largest changes are for NGC 6210 and NGC 6543 for which the M97 temperature scale gives a much lower value of $T_{\rm eff}$ than adopted by P93, and for NGC 2392 and NGC 3242 where the M97 values are much higher than $T_{\rm eff}$ adopted by K97. For the first two stars the revised mass loss rates are more than a factor 10 higher than the old ones. For the second two stars, for which K97 only give upperlimts of $\dot{M}$, the revised upper limits are more than a factor 10 smaller than the old ones.

These considerations show that the derived mass loss rates of CSPN are extremely sensitive to the adopted stellar parameters. Our revised values are at least from a consistent *set of stellar parameters. Whether they represent the* correct *values remains to be seen. The large differences between the effective temperatures quoted in the literature (see Table 3) are not very encouraging.*

The purpose of our study was the investigation of two interesting relations of the modified wind momentum of CSPN. The first one was the relation between Π and L_*, that was found by K97. The second one was the peculiar large separation (or large scatter) in the Π versus L_* plot of the values derived by P93 on the one hand, and those of K97 on the other hand (see Fig. 2), pointed out by Lamers & Cassinelli (1999, Chapt. 2) and by Kudritzki & Puls (2000). Our revisions of the mass loss rates and of the modified wind momentum destroy both relations (see Fig. 6):
– (1) there is no clear dependence of Π on L_* anymore,
– (2) there is no more clear separation between the P93 and K97 data anymore,
– (3) instead, we find that $\dot{M}$ and Π show a strong dichotomy between the young and "cool" Of-type CSPN of $T_{\rm eff} < 60\,000$ K and the older and "hotter" O-type CSPN. This last effect could already be seen in the data of P93 and K97, because both sets contained stars that deviate significantly from the Π versus L_* relation of the other stars (see Sect. 2).

The revised values of the mass loss rates and the modified wind momentum show a large drop somewhere between about 55 000 and 70 000 K. This drop is most likely due to a bi-stability jump in the mass loss rate. The possibility of such a jump was already mentioned by Vink et al. (2001), based on their theoretical wind models.

We conclude that at present there is no observational evidence for the existence of well defined relation between Π *and* L_* *of the CSPN. This implies that at the moment the study of the wind parameters of the CSPN can not be used to derive the distances of these stars.* (The situation might improve if the stellar and wind parameters of the CSPN can be determined more reliably based on the UV spectroscopy of the *LYMAN* satellite.)

7.2. Consequences

The absence of a clear relation between wind momentum and luminosity of CSPN is surprising. The radiation driven wind theory is very successful in explaining the properties of the O-star winds. The overall similarities between the wind properties of CSPN and O-stars, in terms of mass loss rates and terminal velocities strongly suggest that the same mechanisms, i.e. radiation pressure in spectral lines, is driving the wind. So why is there a clear relation for the wind properties of O-stars but not for the CSPN?

The answer is in the uncertainties and possible errors in the determination of the stellar parameters of the CSPN derived from the stellar spectrum or from the evolution tracks.

- If one adopts the stellar parameters derived from the spectra, as was done by Kudritzki et al. (1997), then there is a relation between the modified wind momentum Π and the luminosity as predicted by the radiation driven wind theory with a bi-stability jump around 60 000 K. However, these stellar parameters do not agree with the post-AGB evolution tracks for the kinematic ages of the nebulae. They predict too massive stars for their luminosity, compared to the predicted core mass – luminosity relation of the evolutionary tracks. Moreover, if the strong winds of several CSPN are the consequence of a high luminosity, as predicted by the radiation driven wind theory, these high luminosities would imply a short time since the star left the AGB, according to the evolution theory. This is in disagreement with the kinematic ages of the their nebulae.
- If one adopts the stellar parameters from the post-AGB evolution theory, as was done by Malkov (1997, 1998) and in this paper, then there is no relation between the modified wind momentum and stellar luminosity, contrary to the predictions of the radiation driven wind theory. In that case we have to admit that we do not understand the mechanism for the mass loss of the CSPN. This is difficult to accept because the properties of the O-star winds, which are quite similar to those of the CSPN winds, are well explained by the radiation driven wind theory.

So the question comes down to confidence (or the lack of it) in the predictions of either the post-AGB evolution theory or the radiation driven wind theory. Let us consider their accuracy and identify possible errors.

(a) The evolution of post-AGB stars, and especially the crossing time in the HRD, depends crucially on the time of the superwind phase and on the mass loss rate during the post-AGB phase (e.g. Schönberner 1983; Blöcker 1995). These properties have not been measured, but have been derived from an overall comparison between the predicted and observed dynamical ages of the planetary nebulae. This comparison is severely hampered by the uncertainty in the distances of PN: an error in the distance translates

directly into an error in the radius of the nebula and in its kinematic age. The presence of low luminosity CSPN of $L \simeq 10^2$–$10^3\ L_\odot$ around the galactic center, whose distances are statistically well determined, and whose predicted ages are much longer than the kinematic ages, is an example that the post-AGB evolution predictions may be in error (Pottasch et al. 1988; Pottasch 1990). The fact that several high luminosity CSPN are predicted to evolve more quickly than they actually do is another indication of uncertainties or errors in the predicted post-AGB evolution (Pottasch 1997). So one should not overestimate the accuracy of the post-AGB evolution predictions.

(b) On the other hand, the spectroscopic analysis and the predictions of the radiation driven wind theory also have their limitations. The spectroscopic gravity determination is sensitive to details of the model atmosphere and to the adopted metallicity, which is not well known for CSPN. A comparison between the spectroscopic gravities of O stars in binary systems with independent mass determinations shows that the spectroscopic masses tend to underestimate the gravity and the mass of the stars (Hilditch et al. 1996). Part of this discrepancy might be due to the use of hydrostatic atmosphere models in which wind contamination of the hydrogen and helium lines is not taken into account. Insufficient metal line blanketing in the atmospheric model also tends to give too low spectroscopic gravities and masses (Lanz et al. 1996; Kudritzki & Puls 2000), although this effect may not be large enough to explain the mass discrepancy of the O supergiants. The mass loss rates and wind velocities, predicted by the radiation driven wind theory, depend crucially on the abundances and the degree of ionization of the elements in the wind, as well as on the proper treatment of the photon-wind interactions. Large variations may occur in the abundances of the CSPN stars, of especially He, C, N and O (Pottasch 1997). Puls et al. (2000) and Vink et al. (2001) have shown that for stars with $T_{\rm eff} > 25\,000$ K CNO becomes increasingly more important for the line driving of the wind. This makes the predictions of CSPN mass loss rates and wind velocities sensitive to the variations of these abundances. Vink et al. (1999) have shown that the proper treatment of multiple photon interactions with huge numbers (10^5 to 10^6) of possible transitions in the wind results in higher mass loss rates than predicted by models without multiple scattering. The models used for the wind analysis of the CSPN by Kudritzki et al. (1997) did not include metal line blocking. This may have influenced their derived parameters because the strength of the HeII 4686 line, which is used for determining the temperature and the mass loss rate, is very sensitive to the metal line blocking around 304 Å which is the wavelength of the HeII resonance line (see K97 and Kudritzki & Puls 2000).

We conclude that there is room for improvement in both the predictions of the post-AGB evolution and the radiation driven wind theory for CSPN. The lack of a correlation found between the wind parameters and the luminosity of CSPN, found in this paper, cannot be used as an argument to discard the radiation driven wind theory for the CSPN. On the contrary, the discrepancies found in this paper can be used to improve both the wind theory and the evolution theory, if the distances of PN can be derived more accurately.

Acknowledgements. We thank Mario Perinotto for advice and for hospitality during the stay of the first author in Firenze. We are very grateful to Rolf Kudritzki and Roberto Mendez for critical and constructive comments on an earlier version of this paper.

References

Acker, A., Fresneau, A., Pottasch, S. R., & Jasniewicz, G. 1998, A&A, 337, 253
Blöcker, T. 1995, A&A, 299, 755
Bohlin, R. C., Harrington, J. P., & Stecher, T. P. 1982, ApJ, 252, 635
Castor, J. I., Abbott, D. C., & Klein, R. I. 1975, ApJ, 195, 157
Cerruti-Sola, M., & Perinotto, M. 1989, ApJ, 345, 339
de Koter, A., Heap, S. R., Hubeny, I., & Lanz, T. 1996, in Hydrogen-Deficient Stars, ed. C. S. Jeffery, & U. Heber, ASP Conf. Ser., 96, 141
Gruenwald, R., & Viegas, S. M. 2000, ApJ, 543, 889
Hajian, A. R., Terzian, Y., & Bignell, C. 1995, AJ, 109, 2600
Hilditch, R. W., Harries, T. J., & Bell, S. A. 1996, A&A, 314, 165
Iben, I. 1995, Phys. Rep., 250, 1
Kudritzki, R. P., & Puls, J. 2000, ARA&A, 38, 613
Kudritzki, R. P., Lennon, D. J., & Puls, J. 1995, in Proc. of ESO workshop, Science with the VLT (Springer-Verlag), 246
Kudritzki, R. P., Mendez, R. H., Puls, J., & McCarthy, J. K. 1997, in Planetary Nebulae, ed. H. J. Habing, & H. J. G. L. M. Lamers (Kluwer Acad. Publ.), IAU Symp., 180, 64
Kudritzki, R. P., Puls, J., Lennon, D. J., et al. 1999, A&A, 350, 970
Lamers, H. J. G. L. M., & Casinelli, J. P. 1999, Introduction to Stellar Winds (Cambridge University Press)
Lamers, H. J. G. L. M., & Leitherer, C. 1993, ApJ, 412, 771
Lamers, H. J. G. L. M., Cerruti-Sola, M., & Perinotto, M. 1987, ApJ, 314, 726
Lamers, H. J. G. L. M., Nugis, T., Vink, J. S., & de Koter, A. 2000, in Thermal and ionization aspects of flows from hot stars: Observations and Theory, ed. H. J. G. L. M. Lamers, & A. Sapar, ASP Conf. Ser., 204, 395
Lamers, H. J. G. L. M., de Koter, A., Vink, J. S., & Kudritzki, R. P. 2002, in preparation
Lanz, T. M., de Koter, A., Hubeny, I., & Heap, S. R. 1996, ApJ, 465, 359
Malkov, Y. F. 1997, ARep, 41, No. 6, 760
Malkov, Y. F. 1998, ARep, 42, No. 3, 293
Malkov, Y. F., Golovatyj, V. V., & Rokach, O. V. 1995, Ap&SS, 232, 99
Martin, W. 1994, A&A, 281, 526
Mendez, R. H., Kudritzki, R. P., Herrero, A., Husfeld, D., & Groth, H. G. 1988, A&A, 190, 113
Mendez, R. H., Herrero, A., & Manchado, A. 1990, A&A, 229, 152
Mendez, R. H., Kudritzki, R. P., & Herrero, A. 1992, A&A, 260, 329
Perinotto, M. 1991, ApJS, 76, 687

Perinotto, M. 1993, in Planetary Nebulae, ed. R. Weinberger, & A. Acker, IAU Symp., 155, 57
Perinotto, M., Cerruti-Sola, M., & Lamers, H. J. G. L. M. 1989, ApJ, 337, 382
Pottasch, S. R. 1990, A&A, 236, 231
Pottasch, S. R. 1997, in Planetary Nebulae, ed. H. J. Habing, & H. J. G. L. M. Lamers (Kluwer Acad. Publ.), IAU Symp., 180, 483
Pottasch, S. R., & Acker, A. 1998, A&A, 329, L5
Pottasch, S. R., Bignell, C., Olling, R., & Zijlstra, A. A. 1988, A&A, 205, 248
Preite-Martinez, A. 1993, in Planetary Nebulae, ed. R. Weinberger, & A. Acker, IAU Symp., 155, 65
Preite-Martinez, A., & Pottasch, S. R. 1983, A&A, 126, 31
Puls, J., Kudritzki, R. P., Herrero, A., et al. 1996, A&A, 305, 171
Reed, D. S., Balick, B., Haijan, A. R., et al. 1999, AJ, 118, 2430
Santolaya-Rey, A. E., Puls, J., & Herrero, A. 1997, A&A, 323, 488
Schönberner, D. 1981, A&A, 103, 119
Schönberner, D. 1983, ApJ, 272, 708
Tylenda, R., Stasinska, G., Acker, A., & Stenholm, B. 1994, A&AS, 106, 559
Terzian, Y. 1997, in Planetary Nebulae, ed. H. J. Habing, & H. J. G. L. M. Lamers, IAU Symp., 180, 29
Vink, J. S., de Koter, A., & Lamers, H. J. G. L. M. 1999, A&A, 350, 181
Vink, J. S., de Koter, A., & Lamers, H. J. G. L. M. 2001, A&A, 369, 574
Werner, K., & Koesterke, L. 1992, in The Atmospheres of the Early-Type Stars, ed. U. Heber, & C. S. Jeffery (Berlin: Springer-Verlag), 288
Wood, P. R., & Faulkner, D. J. 1986, ApJ, 307, 659